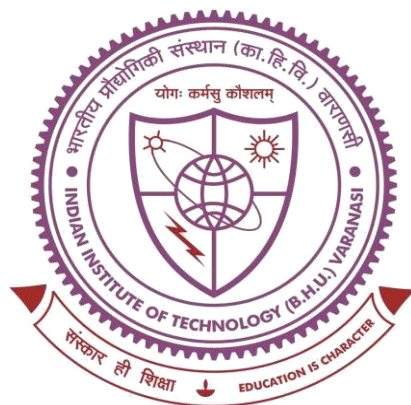


MoSe₂ Nanostructures Based Electrocatalysts for Electrolyzer and Zinc-air Battery



Thesis submitted in partial fulfilment

for the Award of

Doctor of Philosophy

By

Prince Kumar Maurya

SCHOOL OF MATERIALS SCIENCE AND TECHNOLOGY

INDIAN INSTITUTE OF TECHNOLOGY

(BANARAS HINDU UNIVERSITY)

VARANASI – 221005

INDIA

Roll no.: 18111014

Year: 2024



भारतीय
प्रौद्योगिकी
संस्थान
काशी हिन्दू विश्वविद्यालय



INDIAN
INSTITUTE OF
TECHNOLOGY
BANARAS HINDU UNIVERSITY

CERTIFICATE

It is certified that the work contained in the thesis titled *“MoSe₂ Nanostructures Based Electrocatalysts for Electrolyzer and Zinc-air Battery”* by **Prince Kumar Maurya** has been carried out under my supervision and that this work has not been submitted elsewhere for a degree.

It is further certified that the student has fulfilled all the requirements of comprehensive examination, candidacy and SOTA for the award of Ph.D. Degree.

Date: 22-04-2024

Place: Varanasi

Dr. Ashish Kumar Mishra

(Supervisor)

Associate Professor/सह-आचार्य

School of Materials Science & Technology

Indian Institute of Technology

(Banaras Hindu University)

(Banaras Hindu University), Varanasi, काशी हिन्दू विश्वविद्यालय, वाराणसी



भारतीय
प्रौद्योगिकी
संस्थान
काशी हिन्दू विश्वविद्यालय



INDIAN
INSTITUTE OF
TECHNOLOGY
BANARAS HINDU UNIVERSITY

DECLARATION BY THE CANDIDATE

I, "Prince Kumar Maurya", certify that the work embodied in this thesis is my own bonafide work and carried out by me under the supervision of "Dr. Ashish Kumar Mishra" from "July 2018" to "April 2024", at the "School of Material Science and Technology", Indian Institute of Technology (BHU), Varanasi. The matter embodied in this thesis has not been submitted for the award of any other degree/diploma. I declare that I have faithfully acknowledged and given credits to the research workers wherever their works have been cited in my work in this thesis. I further declare that I have not willfully copied any other's work, paragraphs, text, data, results, etc., reported in journals, books, magazines, reports dissertations, theses, etc., or available at websites and have not included them in this thesis and have not cited as my own work.

Date...22-04-2024

Place: Varanasi

Prince

(Prince Kumar Maurya)

CERTIFICATE BY THE SUPERVISOR

This is to certify that the above statement made by the candidate is correct to the best of my knowledge.

Dr. Ashish Kumar Mishra

Dr. Ashish Kumar Mishra
(Supervisor)

School of Materials Science & Technology
Indian Institute of Technology
(Banaras Hindu University)
Varanasi
Indian Institute of Technology
(Banaras Hindu University), Varanasi

Prof. Akhilesh Kumar Singh

Prof. Akhilesh Kumar Singh
(Coordinator)

School of Materials Science & Technology
Indian Institute of Technology
(Banaras Hindu University)
Varanasi

Coordinator/समन्वयक

School of Materials Science & Technology/पदार्थ विज्ञान एवं प्रौद्योगिकी स्कूल
Indian Institute of Technology/भारतीय प्रौद्योगिकी संस्थान
(Banaras Hindu University), Varanasi/काशी हिन्दू विश्वविद्यालय, वाराणसी



भारतीय
प्रौद्योगिकी
संस्थान
काशी हिन्दू विश्वविद्यालय



INDIAN
INSTITUTE OF
TECHNOLOGY
BANARAS HINDU UNIVERSITY



भारतीय
प्रौद्योगिकी
संस्थान
काशी हिन्दू विश्वविद्यालय



INDIAN
INSTITUTE OF
TECHNOLOGY
BANARAS HINDU UNIVERSITY

COPYRIGHT TRANSFER CERTIFICATE

Title of the Thesis: *MoSe₂ Nanostructures Based Electrocatalysts for Electrolyzer and Zinc-air Battery*

Name of the Student: *Prince Kumar Maurya*

Copyright Transfer

The undersigned hereby assigns to the Indian Institute of Technology (Banaras Hindu University) Varanasi all rights under copyright that may exist in and for the above thesis submitted for the award of the “*DOCTOR OF PHILOSOPHY*”.

Date: 22-04-2024

Place: Varanasi

Prince

(Prince Kumar Maurya)

Note: However, the author may reproduce or authorize others to reproduce material extracted verbatim from the thesis or derivative of the thesis for author's personal use provided that the source and the Institute's copyright notice are indicated.

Acknowledgements

Even though the title page of this thesis only lists one name, several people were involved in its acquisition. First and foremost, I want to thank God Almighty for all the privileges and possibilities He has given me throughout my life. I would like to express my sincere gratitude to my esteemed supervisor **Dr. Ashish Kumar Mishra** for all the fruitful scientific discussions and insightful comments throughout my Ph.D. work. Without his constant monitoring, valuable time, guidance and cooperation, I would not have been able to complete my Ph.D. thesis successfully. His supportive nature has significantly fueled my motivation in work. His patience and excitement during my training are beyond description, and I will forever be grateful to him.

I would also like to express my sincere thanks to my RPEC members Prof. Akhilesh Kumar Singh, School of Materials Science & Technology, IIT (BHU) and Dr. Md. Mohammad Imteyaz Ahmad, Department of Ceramic Engineering, IIT (BHU), for their significant scientific discussion and appreciation during the whole journey. I would like to thank present and previous coordinators of School of Materials Science and Technology, IIT (BHU), for providing instrumental facility and cooperation during my Ph.D. I wish to express deep regards to all the teachers of the Department Prof. D. Pandey, Prof. P. Maiti, Prof. R. Prakash, Prof. C. Rath, Prof. A. K. Singh (Coordinator), Dr. C. Upadhyay, Dr. B. N. Pal, Dr. S. K. Mishra, Dr. N. Kumar, Dr. R. Panwar and Dr. A. Kumar for their inspiration and kind support.

With a deep sense of gratitude, I express my sincere thanks to CIFC, IIT (BHU), Varanasi for help in carrying characterization of the synthesized samples. I am also thankful to all the technical, non-teaching as well as office staffs of the School of Material Sciences and Technology, IIT (BHU) Varanasi for their assistance and support whenever required.

My appreciation also goes to my labmates for their great help during my PhD journey- Dr. Bishnu Pada Majee, Dr. Shanu Mishra, Mrs. Ankita Singh, Mr. Jay Deep Gupta, Mr. Rohit Kumar Gupta, Ms. Priyanka Jangra, Mrs. Antima Pandey, Mr. Ankit Raj and my M.Tech juniors- Nilesh, Shweta, Somesh, Shiksha, Vikash, Kundan, Pankaj and Sanghamitra. I am extremely thankful to my friends for making my stay here enjoyable and for their time-to-time encouragement during my Ph. D. journey - Dr. Shubham, Mr. Amit, Mr. Kamal, Mr. Yogesh, Ms. Divya, Ms. Sonam, Mr. Rajnikant, Ms. Rajnandini, Mr. Pawan Ojha, and other whoever helped me in this period. I could not be supposed to have a better friendly environment for my PhD life at IIT (BHU).

Finally, my deepest gratitude to my family, without whom this thesis would not have been possible. I am lucky to thank my younger brother, Mr. Pratish Kumar Maurya, my elder sister, Mrs. Vibha Verma and my cousins Aman and Arun for love, support, happiness and direction in life whenever I needed them. I would also like to express my heartfelt gratitude towards my grandfather- Late Sri Amarnath Singh, for shaping me into what I am today. My heartfelt gratitude is extended to the soul of my life- “my parents”- Mrs. Sadhana Devi and Mr. Ramkesh Singh Maurya for their love, support and blessing at every step of my life that cannot be expressed in words. Most importantly, they inspired me to become an honest and kind-hearted person above all. I genuinely feel that this thesis belongs to them more than to me.

In the end, my sincere gratitude to the DST-India for providing me the INSPIRE fellowship, training, a wonderful learning experience and a chance to collaborate with people with great expertise in the field outside my university. My warm thanks to the CIFC, IIT (BHU) instrumental facility, and the SERB, India for research grant.

(Prince Kumar Maurya)

***Dedicated to my beloved*
*parents***

List of Figures

Figure 1.1 Periodic table showing transition metal and chalcogen elements.....	5
Figure 1.2 Schematic diagram of MoSe ₂ polytypes-1T, 2H, and 3R along with the side views.....	6
Figure 1.3 Schematic showing representation of the different synthesis methods of MoSe ₂	8
Figure 1.4 Schematic diagram for different applications of MoSe ₂	10
Figure 1.5 Schematic of overall water splitting cell.....	11
Figure 2.1 Photograph of the used hydrothermal cell	23
Figure 2.2 Schematic diagram for hydrothermal synthesis of pristine MoSe ₂ nanosheets	24
Figure 2.3 Schematic diagram for <i>in-situ</i> synthesis of MoSe ₂ on CCP and Ni foam substrates.....	25
Figure 2.4 (a)Schematic representation of X-ray diffraction process and (b) XRD pattern for pristine MoSe ₂	28
Figure 2.5 (a) Schematic diagram of SEM and (b) SEM image of pristine MoSe ₂	30
Figure 2.6 (a) Schematic diagram of TEM and (b) TEM image of pristine MoSe ₂	31
Figure 2.7 (a) Schematic representation of the various scattering process: Rayleigh, stokes and anti-stokes Raman scattering, (b) graphic representation of Raman spectrometer and (c) Raman spectrum of MoSe ₂ nanosheets	33
Figure 2.8 (a) Graphic representation of FTIR spectrometer and (b) FTIR spectrum for pristine MoSe ₂ nanosheets.....	34
Figure 2.9 (a) Graphic representation of XPS principle and (b) XPS spectrum for pristine MoSe ₂ nanosheets.....	35
Figure 2.10 Graphic representation of three cell electrochemical setup.....	37
Figure 2.11 (a) Linear voltage sweep with respect to time and (b) LSV curve at different voltage sweep rates.....	38
Figure 2.12 Schematic illustration of typical CV curves.....	39
Figure 2.13 Schematic illustration of typical Nyquist plot for catalytic behavior.....	40
Figure 2.14 Schematic illustration of Galvanostatic charge-discharge behavior of the battery.....	41

Figure 2.15 Photograph of indigenously designed electrolyzer setup showing production of H ₂ and O ₂	42
Figure 2.16 Different components and assembled zinc-air battery.....	43
Figure 3.1 Basic schematic for splitting water into hydrogen and oxygen.....	46
Figure 3.2 (a) HER mechanism in acidic and alkaline condition, (b) Volcano plot showing probable electrocatalysts for HER.....	50
Figure 3.3 SEM images of (a,b) MoSe ₂ -CCP and (c,d) MoSe ₂ -Ni foam electrodes; TEM and HRTEM images of (e,f) MoSe ₂ -CCP and (g,h) MoSe ₂ -Ni foam electrodes.....	54
Figure 3.4 (a) XRD patterns, (b) Raman and (c) FTIR spectra for MoSe ₂ -CCP and MoSe ₂ -Ni foam.....	56
Figure 3.5 (a) Survey spectrum, spectra of (b) Mo 3d and (c) Se 3d for MoSe ₂ -CCP; (d) survey spectrum, spectra of (e) Mo 3d and (f) Se 3d, for MoSe ₂ -Ni foam.....	57
Figure 3.6 CV curves of (a) MoSe ₂ -Ni foam and (b) MoSe ₂ -CCP in 1M KOH; (c) MoSe ₂ -Ni foam and (d) MoSe ₂ -CCP in 0.5M H ₂ SO ₄ at different scan rates, (e) current density plotted against different potential sweep rates.....	58
Figure 3.7 The HER activity of MoSe ₂ -CCP and MoSe ₂ -Ni foam in 1M KOH (a) LSV curves and (b) corresponding Tafel plots at a potential sweep rate of 2 mV s ⁻¹ , including for bare substrates and 20% Pt/C (c) EIS curves at a constant overpotential of -0.2 V vs RHE, (d) the iR corrected LSV curves, (e) corresponding iR corrected Tafel plots and (f) chronoamperometry study at a constant overpotential of -0.2 V vs RHE.....	60
Figure 3.8 The HER activity of MoSe ₂ -CCP and MoSe ₂ -Ni foam in 0.5M H ₂ SO ₄ (a) LSV curves and (b) corresponding Tafel plots at a potential sweep rate of 2 mV s ⁻¹ , including for bare substrates and 20% Pt/C (c) EIS curves at a constant overpotential of -0.2 V vs RHE, (d) the iR corrected LSV curves, (e) corresponding iR corrected Tafel plots and (f) chronoamperometry study at a constant overpotential of -0.2 V vs RHE.....	62
Figure 3.9 (a) SEM, (b) TEM and (c) HRTEM images of MoSe ₂ nanosheets.....	63
Figure 3.10 (a) XRD pattern, (b) Raman and (c) FTIR spectra for MoSe ₂ nanosheets.....	64
Figure 3.11 XPS spectra of pristine MoSe ₂ nanosheets (a) Survey spectrum; Spectra for (b) Mo 3d, and (c) Se 3d	65
Figure 3.12 (a) CV curves at different scan rates, (d) current density plotted against different potential sweep rates for pristine MoSe ₂ nanosheets.....	65
Figure 3.13 HER activity of pristine MoSe ₂ in 1M KOH (a) LSV curve, (b) corresponding Tafel plot (c) EIS spectrum at constant overpotential of -0.2 V vs RHE, (d) The iR corrected LSV curve, (e) corresponding iR corrected Tafel plot, and (f) chronoamperometry study at constant potential of -0.2V vs RHE.....	66
Figure 3.14 (a,b,c) SEM images and (d,e,f) EDS spectra for Ni-MoSe ₂ (5%), Ni-MoSe ₂ (10%), and Ni-MoSe ₂ (20%) nanocomposites, respectively.....	68

Figure 3.15 (a) TEM and (b) higher magnification TEM images of Ni-MoSe ₂ (10%) nanocomposite.....	69
Figure 3.16 (a) XRD patterns, (b) Raman and (c) FTIR spectra for Ni-MoSe ₂ (5%), Ni-MoSe ₂ (10%) and Ni-MoSe ₂ (20%) nanocomposites.....	70
Figure 3.17 (a) Survey spectrum; spectra of (b) Mo 3d, (c) Se 3d and (d) Ni 2p, for Ni-MoSe ₂ (10%) nanocomposite.....	71
Figure 3.18 CV curves of (a) Ni-MoSe ₂ (5%), (b) Ni-MoSe ₂ (10%) and (c) Ni-MoSe ₂ (20%) in 1M KOH at different scan rates, (d) current density plotted against different potential sweep rates.....	72
Figure 3.19 (a) LSV curves, (b) corresponding Tafel plots at scan rates of 2 mV s ⁻¹ , (c) EIS spectra at constant overpotential of -0.2 V vs RHE, (d) The iR corrected LSV curves, (e) corresponding iR corrected Tafel plots and (f) chronoamperometry study at constant potential of -0.2V vs RHE of Ni-MoSe ₂ (5%), Ni-MoSe ₂ (10%) and Ni-MoSe ₂ (20%) nanocomposites in 1M KOH.....	74
Figure 4.1 Conventional OER mechanism in (a) acidic and (b) basic medium.....	78
Figure 4.2 The OER activity of MoSe ₂ -CCP and MoSe ₂ -Ni foam electrodes in 1M KOH electrolyte (a) LSV curves and (b) corresponding Tafel plots at potential sweep rate of 2 mV s ⁻¹ including for bare substrates and RuO ₂ (c) EIS curve at constant overpotential ~1.6 V vs RHE, (d) The iR corrected LSV curves, (e) corresponding iR corrected Tafel plots and (f) chronoamperometry study at constant potential ~1.6 V vs RHE.....	84
Figure 4.3 LSV curves of (a) MoSe ₂ -CCP and (b) MoSe ₂ -Ni foam at a scan rate of 2 mV s ⁻¹ in 0.5M H ₂ SO ₄	86
Figure 4.4 Electrochemical OER activity of MoSe ₂ , (a) LSV curve at a scan rate of 2 mV s ⁻¹ , (b) corresponding Tafel plot, (c) EIS plot at 1.574 V vs RHE, (d) 90% iR corrected OER LSV curve of MoSe ₂ at a scan rate of 2 mV s ⁻¹ , (e) iR corresponding Tafel plot, (f) chronoamperometric curve for prepared sample to observe stability of electrocatalytic activity.....	87
Figure 4.5 (a) CV curves at different scan rates, (b) $\Delta J/2=(J_a-J_c)/2$ current density plotted against different potential sweep rates for pristine MoSe ₂ nanosheets.	89
Figure 4.6 The OER activity of Ni-MoSe ₂ (5%), Ni-MoSe ₂ (10%) and Ni-MoSe ₂ (20%) nanocomposites in 1M KOH electrolyte (a) LSV curves and (b) corresponding Tafel plots at potential sweep rate of 2 mV s ⁻¹ , (c) EIS curve at constant overpotential ~1.6 V vs RHE, (d) The iR corrected LSV curves, (e) corresponding iR corrected Tafel plots and (f) chronoamperometry study at constant potential ~1.6 V vs RHE.....	91
Figure 4.7 SEM, TEM and higher magnification TEM images of (a-c) NiCo ₂ O ₄ /NiO and (d-f) NiCo ₂ O ₄ /NiO-MoSe ₂ hybrid nanostructure, respectively.....	92
Figure 4.8 (a) XRD patterns (b) Raman and (c) FTIR spectra of NiCo ₂ O ₄ /NiO and NiCo ₂ O ₄ /NiO-MoSe ₂ hybrid nanostructure	94

Figure 4.9 XPS spectra of NiCo ₂ O ₄ /NiO-MoSe ₂ hybrid nanostructures (a) Survey spectrum; Spectrum for (b) Mo 3d, (c) Se 3d, (d) Ni 2p, (e) Co 2p, and (f) O 1s.....	95
Figure 4.10 (a) Comparison of the LSV curves of MoSe ₂ , NiCo ₂ O ₄ /NiO, and NiCo ₂ O ₄ -MoSe ₂ hybrid nanostructure in 1M KOH at a scan rate of 2 mV s ⁻¹ for OER study, (b) Corresponding Tafel plots, (c) Comparison of EIS plots at 1.574 V vs RHE, (d) iR corrected OER LSV curve, (e) iR corresponding Tafel plots and (f) Chronoamperometric curves for prepared samples to observe stability of electrocatalytic activity.....	97
Figure 4.11 CV curves at different scan rates of (a) NiCo ₂ O ₄ /NiO-MoSe ₂ , hybrid nanostructure and (b) NiCo ₂ O ₄ /NiO; (c) corresponding electrochemical double-layer capacitances (C _{dl}).....	99
Figure 4.12 (a,c) SEM and (b,d) TEM images for CoFe ₂ O ₄ and CoFe ₂ O ₄ -MoSe ₂ hybrid nanostructures, respectively.....	100
Figure 4.13 (a) XRD patterns, (b) Raman and (c) FTIR spectra of CoFe ₂ O ₄ and CoFe ₂ O ₄ -MoSe ₂ hybrid nanostructure.....	102
Figure 4.14 XPS spectra of (a) survey spectra, (b) Co 2p, (c) Fe 2p, (d) O 1s, (e) Mo 3d and (f) Se 3d for CoFe ₂ O ₄ -MoSe ₂ hybrid nanostructure.....	103
Figure 4.15 (a) LSV curves, (b) corresponding Tafel plots at potential sweep rates of 2 mV s ⁻¹ , (c) EIS curves, (d) 90% iR corrected LSV curves, (e) iR corrected corresponding Tafel plots, (f) Chronoamperometry curves at a constant potential of 1.55 V vs RHE for CoFe ₂ O ₄ and CoFe ₂ O ₄ -MoSe ₂ hybrid nanostructure prepared electrocatalysts in 1M KOH.....	105
Figure 4.16 CV curves of (a) CoFe ₂ O ₄ , (b) CoFe ₂ O ₄ -MoSe ₂ hybrid nanostructure at different scan rates and (c) corresponding electrochemical double-layer capacitance (C _{dl}).....	107
Figure 4.17 (a,c) SEM and (b,d) TEM images for NiFe ₂ O ₄ and NiFe ₂ O ₄ -MoSe ₂ hybrid nanostructures, respectively.....	108
Figure 4.18 (a) XRD patterns, (b) Raman and (c) FTIR spectra of NiFe ₂ O ₄ and NiFe ₂ O ₄ -MoSe ₂ hybrid nanostructure.	110
Figure 4.19 XPS spectra for NiFe ₂ O ₄ -MoSe ₂ hybrid nanostructure (a) survey spectrum, spectra for (b) Ni 2p, (c) Fe 2p, (d) O 1s, (e) Mo 3d and (f) Se 3d.....	111
Figure 4.20 (a) LSV curves, (b) corresponding Tafel plots at potential sweep rates of 2 mV s ⁻¹ , (c) EIS curves, (d) 90% iR corrected LSV curves (e) corresponding iR corrected Tafel plots and (f) chronoamperometry curves at a constant potential of 1.55 V vs RHE for NiFe ₂ O ₄ and NiFe ₂ O ₄ -MoSe ₂ hybrid nanostructure in 1M KOH.....	113
Figure 4.21 CV curves at different scan rates for (a) NiFe ₂ O ₄ , (b) NiFe ₂ O ₄ -MoSe ₂ hybrid nanostructure and (c) corresponding electrochemical double-layer capacitance (C _{dl}).....	115
Figure 5.1 Schematic diagram of overall water splitting.....	119
Figure 5.2 (a) Schematic and (b) photograph of indigenously designed electrolyzer setup for production of H ₂ and O ₂	126

Figure 5.3 Performance of MoSe₂-CCP and MoSe₂-Ni foam based electrolyzers, (a) LSV curves at a potential scan rate of 2 mVs⁻¹, (b) chronoamperometric measurement at a constant potential of 1.6 V vs RHE, theoretically calculated and experimentally measured H₂ and O₂ gas vs time for overall water splitting with (c) MoSe₂-CCP and (d) MoSe₂-Ni foam based electrolyzers; Faradaic efficiency of (e) MoSe₂-CCP, (f) MoSe₂-Ni foam based electrolyzers for H₂ and O₂.....128

Figure 5.4 Performance of pristine MoSe₂ based electrolyzer, (a) LSV curves at a potential scan rate of 2 mVs⁻¹, (b) chronoamperometric measurement at a constant potential of 1.6 V vs RHE, (c) theoretically calculated and experimentally measured H₂ and O₂ gas vs time for overall water splitting and (d) Faradaic efficiency of electrolyzers for H₂ and O₂.....130

Figure 5.5 Performance of Ni-MoSe₂ (5%), Ni-MoSe₂ (10%) and Ni-MoSe₂ (20%) based electrolyzers, (a) LSV curves at a potential scan rate of 2 mVs⁻¹, (b) chronoamperometric measurement at a constant potential of 1.6 V vs. RHE; theoretically calculated and experimentally measured H₂ and O₂ gas vs time for overall water splitting with (c) Ni-MoSe₂ (5%), (d) Ni-MoSe₂ (10%) and (e) Ni-MoSe₂ (20%) based symmetric electrolyzers; Faradaic efficiency of (f) Ni-MoSe₂ (5%), (g) Ni-MoSe₂ (10%) and (h) Ni-MoSe₂ (20%) nanocomposites based electrolyzers for H₂ and O₂.....133

Figure 6.1 (a) Schematic diagram of a typical metal-air battery and (b) theoretically estimated energy densities of various types of metal-air batteries139

Figure 6.2 (a) Schematic of a typical zinc-air battery and (b) photograph of fabricated zinc-air battery.....145

Figure 6.3 (a) OCP curve, (b) Specific capacity curve at current density of 10 mA cm⁻², (c) discharge voltage curve and corresponding power density plot and (d) charging-discharging curves at a current density of 10 mA cm⁻² for fabricated zinc-air battery using MoSe₂ nanosheets.....146

Figure 6.4 Raman spectra for MoSe₂ nanosheets-based air cathode before and after cyclic durability of battery stability.....149

Figure 6.5 (a) OCP curve, (b) Specific capacity curve at current density of 10 mA cm⁻², (c) discharge voltage curves and corresponding power density plots and (d) charging-discharging curves at a current density of 10 mA cm⁻² for fabricated zinc-air batteries.....147

Figure 6.6 Raman spectra for NiCo₂O₄/NiO-MoSe₂ hybrid nanostructure-based air cathode before and after cyclic durability of battery stability.....150

Figure 6.7 (a) Open circuit potentials, (b) constant discharge curves at 10 mA cm⁻², (c) galvanodynamic discharge and power density curves, (d) cyclic stability curves of 5 min charge and 5 min discharge at 10 mA cm⁻² of CoFe₂O₄ and CoFe₂O₄-MoSe₂ hybrid nanostructure based zinc-air batteries151

Figure 6.8 Raman spectra for CoFe₂O₄-MoSe₂ hybrid nanostructure-based air cathode before and after cyclic durability of battery stability.....152

Figure 6.9 (a) Open circuit potentials, (b) constant discharge curves at 10 mA cm⁻², (c) galvanodynamic discharge and power density curves, (d) cyclic stability curves of 5 min charge

and 5 min discharge at 10 mA cm^{-2} of NiFe_2O_4 and $\text{NiFe}_2\text{O}_4\text{-MoSe}_2$ hybrid nanostructure based zinc-air batteries.....153

Figure 6.10 Raman spectra for $\text{NiFe}_2\text{O}_4\text{-MoSe}_2$ hybrid nanostructure-based air cathode before and after cyclic durability of battery stability.....154

List of Tables

Table 3.1 The comparative performance summary of HER activity of our studied materials...	75
Table 4.1 The comparative performance summary of OER activity of studied materials...	116
Table 5.1 The comparative electrolyzer performance summary using our studied materials.....	134
Table 6.1 The comparative performance summary of rechargeable zinc-air batteries with other literature reports.....	155

List of Abbreviations

MoSe ₂	Molybdenum Diselenide
MoS ₂	Molybdenum Disulfide
TMDCs	Transition metal dichalcogenide
HER	Hydrogen Evolution Reaction
OER	Oxygen Evolution Reaction
RHE	Reversible Hydrogen Electrode
CCP	Conducting carbon paper
MABs	Metal Air batteries
XRD	X-ray Diffraction
SEM	Scanning Electron Microscope
TEM	Transmission Electron Microscope
FTIR	Fourier-transform infrared spectroscopy
LSV	Linear Sweep Voltammetry
CV	Cyclic voltammetry
GCD	Galvanostatic Charge-discharge
EIS	Electrochemical Impedance Spectroscopy
CPE	Constant Phase Element
HR	High Resolution
2D	Two Dimensional
CVD	Chemical vapor deposition
ECSA	Electrochemical active surface area

List of Symbols

η	Overpotential
$^{\circ}\text{C}$	Degree Celsius
F	Faraday constant
eV	Electron volt
%	Percentage
C_d	Specific capacity
I_d	Discharge current density
mA	Milli ampere
ΔT	Discharge time
m_{zn}	Consumed mass of zinc
E_d	Energy density
WL^{-1}	Watt per litter
Wh kg^{-1}	Watt hour per kilogram
V	Volt
P_d	Power density
V_d	Discharge working potential
Pt	Platinum
Zn	Zinc
G°	Gibbs free energy
R_s	Series resistance
R_{ct}	Charge transfer resistance
Li	Lithium
E_{op}	Overall potential
E_{rev}	Reversible thermodynamic potential
Ni	Nickle

Table of Contents

<i>Certificate</i>	<i>iii</i>
<i>Declaration by the Candidate</i>	<i>v</i>
<i>Copyright Transfer Certificate</i>	<i>vii</i>
<i>Acknowledgements</i>	<i>ix</i>
<i>Table of Contents</i>	<i>xiii</i>
<i>List of Figures</i>	<i>xix</i>
<i>List of Tables</i>	<i>xxv</i>
<i>List of Abbreviations</i>	<i>xxvii</i>
<i>List of Symbols</i>	<i>xxix</i>
<i>Preface</i>	<i>xxxi</i>
Chapter 1 Introduction and Literature Survey	1-20
1.1 Introduction.....	1
1.2 Molybdenum Disulfide (MoSe ₂).....	5
1.3 Properties of MoSe ₂	6
1.4 Synthesis of MoSe ₂	8
1.5 Applications of MoS ₂ nanostructures.....	10
1.5.1 MoSe ₂ for HER.....	11
1.5.2 MoSe ₂ for OER.....	14
1.5.3 MoSe ₂ for aqueous alkaline electrolyzer.....	15
1.5.4 MoSe ₂ for Zinc air battery.....	17
1.6 Scope and objectives of the present work.....	19
Chapter 2 Synthesis and Characterization Techniques	21-43
2.1 Materials Synthesis.....	22
2.1.1 Hydrothermal synthesis of nanostructures.....	22
2.1.1.1 Precursor required for preparation of desired materials.....	23
2.1.1.2 Synthesis of pristine MoSe ₂ nanosheets.....	23
2.1.1.3 Synthesis of <i>in-situ</i> grown vertical MoSe ₂ over different substrates.....	24
2.1.1.4 Synthesis of CoFe ₂ O ₄	25
2.1.1.5 Synthesis of NiCo ₂ O ₄ /NiO.....	25

2.1.1.6	Synthesis of NiFe ₂ O ₄	25
2.1.1.7	Synthesis of CoFe ₂ O ₄ -MoSe ₂ hybrid nanostructure.....	26
2.1.1.8	Synthesis of NiCo ₂ O ₄ /NiO-MoSe ₂ hybrid nanostructure.....	26
2.1.1.9	Synthesis of NiFe ₂ O ₄ -MoSe ₂ hybrid nanostructure	26
2.1.1.10	Synthesis of Ni decoration MoSe ₂ nanocomposites.....	27
2.2	Characterization techniques.....	27
2.2.1	X-ray diffraction.....	27
2.2.2	Scanning electron microscopy (SEM).....	29
2.2.3	Transmission electron microscopy (TEM).....	30
2.2.4	Raman Spectroscopy.....	32
2.2.5	Fourier transform infrared (FTIR) spectroscopy.....	33
2.2.6	X-ray photoelectron spectroscopy (XPS).....	34
2.2.7	Electrochemical techniques.....	35
2.2.7.1	Linear sweep voltammetry (LSV)	37
2.2.7.2	Cyclic voltammetry (CV)	38
2.2.7.3	Electrochemical impedance spectroscopy (EIS).....	39
2.2.7.4	Galvanostatic charge-discharge measurement	40
2.2.8	Experimental details for electrochemical measurements	41
2.2.9	Design of aqueous alkaline electrolyzer.....	42
2.2.10	Design of zinc-air battery.....	43
Chapter 3	Hydrogen Evolution Reaction Study using MoSe₂ based Nanomaterials as Electrodes	45-76
3.1	Introduction.....	45
3.1.1	Reactions involved in HER process	47
3.1.2	Reaction mechanism for HER	48
3.1.2.1	HER reaction in acidic medium	49
3.1.2.2	HER reaction in alkaline medium	49
3.2	Performance evolution index for electrocatalyst.....	51
3.2.1	Overpotential (η).....	51
3.2.2	Tafel slope and exchange current density.....	52
3.2.3	Electrochemical impedance spectroscopy (EIS) measurements.....	52

3.3	Electrocatalyst for hydrogen production	52
3.4	Results and discussion	53
3.4.1	<i>In-situ</i> grown MoSe ₂ over different substrates as binder free electrodes for HER.....	53
3.4.1.1	Characterization of in-situ grown MoSe ₂ over substrate.....	53
3.4.1.2	Electrochemical characterization.....	58
3.4.2	Pristine MoSe ₂ nanosheets for HER.....	63
3.4.2.1	Characterization of pristine MoSe ₂	63
3.4.2.2	Electrochemical characterization.....	65
3.4.3	Ni decorated MoSe ₂ nanocomposites as electrode for HER	67
3.4.3.1	Characterization of Ni decorated over MoSe ₂	67
3.4.3.2	Electrochemical characterization	71
3.5	Conclusions.....	75

Chapter 4 Oxygen Evolution Reaction Study using MoSe₂ based Nanomaterials as Electrodes77-117

4.1	Introduction.....	77
4.2	Reaction mechanism for OER.....	78
4.2.1	OER process in acidic medium	79
4.2.2	OER process in basic medium	79
4.3	Performance evolution index for electrocatalyst	80
4.3.1	Overpotential (η).....	80
4.3.2	Tafel slope and exchange current density	80
4.3.3	Electrochemical impedance spectroscopy (EIS) measurements.....	80
4.3.4	Number of electrochemical active sites	81
4.4	Results and discussion	82
4.4.1	<i>In-situ</i> grown MoSe ₂ over different substrate as binder free electrodes for OER.....	82
4.4.1.1	Characterization of binder free MoSe ₂ electrodes.....	82
4.4.1.2	Electrochemical characterization.....	82
4.4.2	Pristine MoSe ₂ as electrocatalyst for OER	86

4.4.2.1	Electrochemical characterization.....	86
4.4.3	Ni decorated MoSe ₂ as electrode for OER.....	89
4.4.3.1	Electrochemical characterization.....	89
4.4.4	NiCo ₂ O ₄ /NiO-MoSe ₂ hybrid nanostructure as electrode for OER	92
4.4.4.1	Characterization of NiCo ₂ O ₄ /NiO-MoSe ₂ hybrid nanostructure....	92
4.4.4.2	Electrochemical characterization.....	96
4.4.5	CoFe ₂ O ₄ -MoSe ₂ hybrid nanostructure as electrode for OER.....	99
4.4.5.1	Characterization of CoFe ₂ O ₄ -MoSe ₂ hybrid nanostructure.....	100
4.4.5.2	Electrochemical characterization.....	104
4.4.6	NiFe ₂ O ₄ -MoSe ₂ hybrid nanostructure as electrode for OER.....	107
4.4.6.1	Characterization of NiFe ₂ O ₄ -MoSe ₂ hybrid nanostructure.....	108
4.4.6.2	Electrochemical characterization.....	112
4.5	Conclusion.....	117
Chapter 5	MoSe₂ based Nanomaterials as Electrodes for Electrolyzer.....	119-135
5.1	Introduction.....	119
5.1.1	Types of electrolyzer.....	121
5.2	Performance evolution index for electrolyzer:.....	122
5.2.1	Overpotential (η).....	123
5.2.2	Faradaic efficiency.....	123
5.3	Reaction mechanism for overall water splitting::.....	124
5.4	Electrocatalysts for electrolyzer.....	124
5.5	Assembly of designed electrolyzer	125
5.6	Result and discussion.....	126
5.6.1	<i>In-situ</i> grown MoSe ₂ over different substrate as electrode for alkaline water electrolyzer.....	126
5.6.1.1	Electrochemical characterization	127
5.6.2	Pristine MoSe ₂ nanosheets as electrode for alkaline water electrolyzer....	129
5.6.2.1	Performance of electrolyzer for overall water splitting	129
5.6.3	Ni decorated MoSe ₂ nanosheets as electrode for alkaline water electrolyzer.....	130
5.6.3.1	Performance of electrolyzer for overall water splitting	131

5.7 Conclusions.....	134
Chapter 6 Zinc-air Batteries using MoSe₂ based Nanomaterials as Air cathode	137-156
6.1 Introduction.....	137
6.1.1 Battery performance analysis	141
6.1.1.1 Open circuit potential.....	141
6.1.1.2 Galvanostatic full-discharge.....	141
6.1.1.3 Galvanodynamic discharge polarization.....	142
6.1.1.4 Galvanostatic cycling.....	143
6.1.1.5 Role of electrocatalyst in rechargeable zinc-air batteries.....	143
6.2 Result and discussion.....	145
6.2.1 Assembly of zinc-air battery	145
6.2.2 Zinc-air battery performance using pristine MoSe ₂ as air cathode	146
6.2.3 Zinc-air battery performance using NiCo ₂ O ₄ /NiO-MoSe ₂ hybrid nanostructure as air cathode.....	148
6.2.4 Zinc-air battery performance using CoFe ₂ O ₄ -MoSe ₂ hybrid nanostructure as air cathode.....	150
6.2.5 Zinc-air battery performance using NiFe ₂ O ₄ -MoSe ₂ hybrid nanostructure as air cathode.....	152
6.3 Conclusions.....	156
Chapter 7 Conclusion and Future Scope of the Work.....	157-160
7.1 Conclusions.....	157
7.2 Future scope of the work.....	159
References.....	161
List of Patents, Publications, and Book Chapters.....	181
Schools/Workshops/Conferences Attended	183

Preface

Molybdenum diselenide (MoSe_2) is one of the widely studied materials of the transition metal dichalcogenide family, having fascinating properties such as high conductivity, semiconducting characteristics, high surface area, electrocatalytic activity and good stability in acidic/basic medium. These attractive feature characteristics allow MoSe_2 nanostructures to be used in energy generation and storage applications. The present thesis entitled “ **MoSe_2 Nanostructures Based Electrocatalysts for Electrolyzer and Zinc-air Battery**” is focused on the synthesis of pristine MoSe_2 , bimetal oxides- MoSe_2 hybrid nanostructures and Ni decorated MoSe_2 nanocomposites via hydrothermal technique for hydrogen evolution reaction (HER), oxygen evolution reaction (OER), Electrolyzer, and zinc-air battery applications. The morphology and structure of the synthesized samples have been confirmed through Scanning electron microscopy (SEM), Transmission electron microscopy (TEM) and X-ray diffraction (XRD) techniques. We have also performed Raman and Fourier transform infrared (FTIR) spectroscopy techniques to confirm the vibrational characteristics of prepared samples. The X-ray photoelectron spectroscopy (XPS) has been performed to analyze oxidation states of different elements in pristine MoSe_2 , bimetal oxides- MoSe_2 hybrid nanostructures and Ni decorated MoSe_2 nanocomposite. We have further elucidated the electrocatalytic activity of prepared samples through different electrochemical measurements such as cyclic voltammetry (CV), linear sweep voltammetry (LSV), electrochemical impedance spectroscopy (EIS) and chronoamperometry for HER and OER. Further, we have designed electrolyzer and Zinc air battery cells using prepared electrocatalysts and studied their performance.

In-situ grown MoSe_2 over Ni foam (MoSe_2 -Ni foam) electrode shows low overpotential $\eta_{10} \sim 100$ mV and Tafel slope ~ 73 mV dec^{-1} in 1M KOH for HER, while *in-situ* grown MoSe_2 over conducting carbon paper (MoSe_2 -CCP) electrode displays $\eta_{10} \sim 143$ mV and Tafel's slope ~ 53 mV dec^{-1} in 0.5M H_2SO_4 . The better performance of binder-free MoSe_2 -Ni foam and